

A Plasmid-Borne System To Assess the Excision and Integration of Staphylococcal Cassette Chromosome *mec* Mediated by CcrA and CcrB

Lei Wang,^a Mostafa H. Ahmed,^b Martin K. Safo,^b Gordon L. Archer^a

Department of Internal Medicine, Division of Infectious Diseases, School of Medicine, Virginia Commonwealth University, Richmond, Virginia, USA^a; Institute for Structural Biology and Drug Discovery, Department of Medicinal Chemistry, School of Pharmacy, Virginia Commonwealth University, Richmond, Virginia, USA^b

ABSTRACT

Resistance to methicillin and other β -lactam antibiotics in staphylococci is due to *mecA*, which is carried on a genomic island, staphylococcal cassette chromosome *mec* (SCC*mec*). The chromosomal excision and integration of SCC*mec* are mediated by the site-specific recombinase CcrAB or CcrC, encoded within this element. A plasmid-borne system was constructed to assess the activities of CcrA and CcrB in the excision and integration of SCC*mec* in *Escherichia coli* and *Staphylococcus aureus*. The excision frequency in *E. coli* mediated by CcrAB from methicillin-resistant *S. aureus* (MRSA) strain N315 was only 9.2%, while the integration frequency was 31.4%. In *S. aureus* the excision and integration frequencies were 11.0% and 18.7%, respectively. Truncated mutants identified the N-terminal domain of either CcrB or CcrA to be necessary for both integration and excision, while the C-terminal domain was important for recombination efficiency. Site-directed mutagenesis of the N-terminal domain identified S11 and R79 of CcrA and S16, R89, T149, and R151 of CcrB to be residues essential for catalytic activities, and the critical location of these residues was consistent with a model of the tertiary structure of the N terminus of CcrA and CcrB. Furthermore, CcrAB and CcrC, cloned from a panel of 6 methicillin-resistant *S. aureus* strains and 2 methicillin-resistant *Staphylococcus epidermidis* strains carrying SCC*mec* types II, IV, and V, also catalyzed integration at rates 1.3 to 10 times higher than the rates at which they catalyzed excision, similar to the results from N315. The tendency of SCC*mec* integration to be favored over excision may explain the low spontaneous excision frequency seen among MRSA strains.

IMPORTANCE

Spontaneous excision of the genomic island (SCC*mec*) that encodes resistance to beta-lactam antibiotics (methicillin resistance) in staphylococci would convert a methicillin-resistant strain to a methicillin-susceptible strain, improving therapy of difficult-to-treat infections. This study characterizes a model system by which the relative frequencies of excision and integration can be compared. Using a plasmid-based model for excision and integration mediated by the recombinases CcrA and CcrB, integration occurred at a higher frequency than excision, consistent with the low baseline excision frequency seen in most strains. This model system can now be used to study conditions and drugs that may raise the SCC*mec* excision frequency and generate strains that are beta-lactam susceptible.

Staphylococcus aureus is a leading cause of infection in hospitals and communities throughout the world. The treatment for such infections has become increasingly difficult as a result of the development of resistance to multiple antibiotics. The multiresistance phenotype in *S. aureus* is built around the acquisition of resistance to beta-lactam antibiotics (resulting in methicillin-resistant *S. aureus* [MRSA]), mediated by the gene *mecA*, which encodes a beta-lactam target (PBP 2a) resistant to beta-lactam inactivation. *mecA* is carried on a mobile genomic island, staphylococcal cassette chromosome *mec* (SCC*mec*) (1). At least 11 types of SCC*mec* (types I to XI), ranging from 22 kb to >60 kb, have been described by typing based on the *mec* and *ccr* complexes (2; http://www.sccmec.org/Pages/SCC_TypesEN.html). SCC*mec* integrates into and excises from the chromosome at specific DNA sites (*att*), with integration and excision being catalyzed by a group of serine recombinases, CcrAB and CcrC, carried by the element (3–6). Two pairs of *att* sites are required for SCC*mec* integration (*attB* and *attS*) and excision (*attR* and *attL*) (6). All of the *att* sites share a conserved 8-base core region, required for CcrB DNA binding, with variable flanking sequences that determine the insertion frequency (6).

Serine recombinases catalyze site-specific recombination and play an essential role in the movement of genetic elements, such as bacteriophages, transposons, and large genomic islands (7, 8). For some serine recombinases, there are two different genes for excision and integration, such as phage integrase and phage directionality factor Xis for excision (9–14). Other recombinases, such as TndX from the *Clostridium difficile* tetracycline resistance element (15, 16), me-

Received 29 January 2015 Accepted 30 May 2015

Accepted manuscript posted online 8 June 2015

Citation Wang L, Ahmed MH, Safo MK, Archer GL. 2015. A plasmid-borne system to assess the excision and integration of staphylococcal cassette chromosome *mec* mediated by CcrA and CcrB. *J Bacteriol* 197:2754–2761. doi:10.1128/JB.00078-15.

Editor: O. Schneewind

Address correspondence to Gordon L. Archer, garcher@vcu.edu.

Supplemental material for this article may be found at <http://dx.doi.org/10.1128/JB.00078-15>.

Copyright © 2015, American Society for Microbiology. All Rights Reserved.

doi:10.1128/JB.00078-15

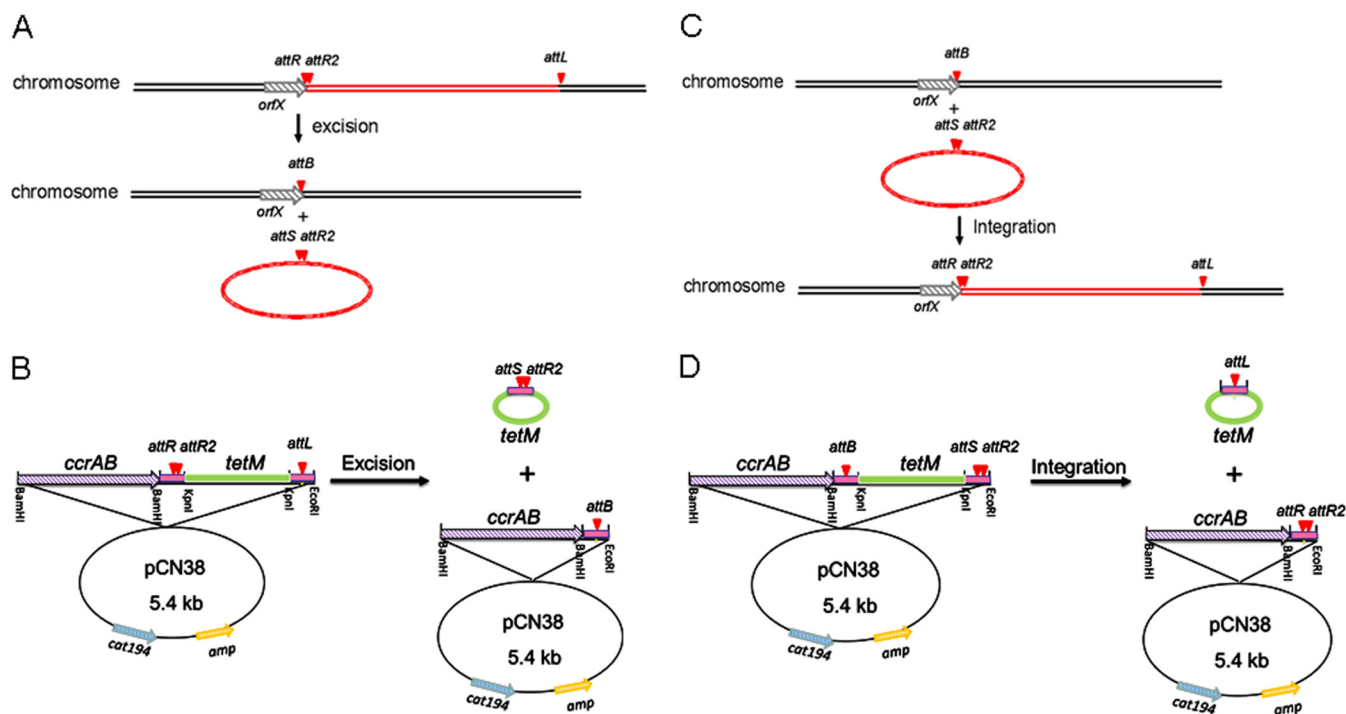


FIG 1 Schematic diagram of the excision and integration of chromosome and model plasmids. (A and C) Schematic diagrams of excision and integration of SCC_{mec}. Black and red double lines, the chromosome and SCC_{mec}, respectively; arrows, the *orfX* gene; arrowheads, *att* sites. (B and D) Schematic diagrams of excision and integration of model plasmids. Both of the plasmids were derived from a chloramphenicol-resistant *E. coli*-*S. aureus* shuttle vector, pCN38. Green, a tetracycline resistance gene (*tetM*), flanked with a pair of 0.6-kb *att* site-containing fragments in a direct orientation; purple arrows, a copy of *ccrAB* genes from MRSA or MRSE strains; blue arrows, a chloramphenicol resistance gene (*cat194*); yellow arrows, an ampicillin resistance gene (*amp*).

mediate both excision and integration. CcrAB and CcrC are examples of large serine recombinases that belong to the latter group. While CcrC is a single protein that carries out both activities, the two proteins CcrA and CcrB must interact in a precise ratio to mediate either integration or excision (4–6). Our previous data showed that CcrB is the major DNA-binding protein, while CcrA is required to direct the complex to the *attB* integration site (5, 6). However, recent data from Misiura et al. (17) demonstrated weak DNA-binding activity for CcrA as well. Most of our previous work has focused on the roles of CcrA and CcrB in integration by putting a gene(s) encoding one or both of these proteins on a temperature-sensitive plasmid, measuring the frequency of integration into chromosomal *att* sites, and scoring for antibiotic resistance after growth at the nonpermissive temperature for plasmid replication. However, we have not previously assessed the relative frequency of integration versus excision. Stojanov et al. (18) found a very low frequency of spontaneous SCC_{mec} excision (10^{-5} to 10^{-6}) in *S. aureus*, a frequency that we have also observed (L. Wang, unpublished observations). This suggests either that excision rarely occurred or that excision occurred frequently but was followed by immediate reintegration. The following study was performed in an attempt to measure the relative rates of SCC_{mec} excision and integration mediated by CcrAB and CcrC, using a two-plasmid system in both *Escherichia coli* and *S. aureus*, and the contribution of the various domains of each of the two proteins CcrA and CcrB to the process.

MATERIALS AND METHODS

Strains and media. All of the strains used in this work are listed in Table S1 in the supplemental material. Staphylococcal strains were cultured in

tryptic soy broth (TSB; Thermo Scientific, Waltham, MA). *E. coli* TOP10 (Invitrogen, Carlsbad, CA) was used for gene cloning. The antibiotics and concentrations used were as follows: 100 μ g/ml ampicillin (Ap) for selection of *E. coli* strains following transformation and 10 μ g/ml chloramphenicol (Cml) and 5 μ g/ml tetracycline (Tet) for selection of *S. aureus* strains following electroporation (19).

Plasmid model for excision and integration. Each excision/integration model plasmid contained a tetracycline resistance gene (*tetM*) flanked by a pair of *att* sites in direct orientation and by a copy of a *ccr* gene driven by its own promoter (*ccrA*, *ccrB*, *ccrAB*, or *ccrC*) (Fig. 1B and D). The *ccrAB* genes for all studies were from strain N315 (see Table S1 in the supplemental material), unless otherwise specified. The *ccrC* gene was from strain WBG8318 (see Table S1 in the supplemental material). All of the *att* site-containing fragments were 600 bp, with the *att* core sequence being in the middle. Recombination between *attR* and *attL* was defined as excision, and that between *attB* and *attS* was defined as integration. Recombination mediated by Ccr proteins was identified by the deletion of the *tetM* gene. As recombination occurred, a 3.1-kb fragment containing *tetM* was deleted, reducing the size of the plasmid. Recombination was identified and quantified by first cleaving the plasmid with BamHI, releasing the *ccr* gene(s), and leaving the backbone containing either the unexcised *tetM*-containing fragment (9 kb) or the excised fragment (6 kb). This size shift was easily detected by agarose gel electrophoresis. The relative recombination frequency (RF) was determined by the following equation: RF (in percent) = molecular number of excised bands / (molecular number of excised bands + molecular number of unexcised bands).

The molecular number of each DNA fragment was calculated to be the relative band density divided by the molecular weight. The relative band density on the gel image was determined by ImageJ software (<http://imagej.nih.gov/ij/>), and the molecular weight was calculated as follows (20): approximate molecular weight of double-stranded DNA (dsDNA; in grams per mole) = numbers of nucleotides \times 660 g/mol.

The loss of tetracycline resistance was not a useful marker for recombination because in a multicopy plasmid system recombination could occur in some fraction of the plasmid population but not the entire population, resulting in lower numbers for excision and integration. However, the results were in the same direction and the differences mirrored those seen with the *E. coli* plasmid system. Thus, since the plasmid size system did not work well in *S. aureus*, we used tetracycline susceptibility to confirm in *S. aureus* some of the observations made in *E. coli*.

The plasmids described above were constructed as follows. A chloramphenicol-resistant *E. coli*-*S. aureus* shuttle vector, pCN38 (21), was the backbone for all constructs. The ~0.6-kb fragments containing *attR* and *attL* sites were amplified from the N315 genome with primers attR-F-BamHI and attR-R-KpnI and primers attL-F-KpnI and attL-R-EcoRI, respectively. The 0.6-kb *attB* and *attS* fragments were amplified from N315/pWA46 (5) with primers attB-F-BamHI and attB-R-KpnI and primers attS-F-KpnI and attS-R-EcoRI, respectively. A 2.5-kb *tetM* gene was amplified from pCN36 (21) using the primers tetM-F-KpnI and tetM-R-KpnI. pWA340/pWA341 were constructed by the use of three PCR products cloned into pCN38 one by one: an *attR*- or *attB*-containing fragment at the BamHI/KpnI site, an *attL*- or *attS*-containing fragment at the KpnI/EcoRI site, and then a *tetM* fragment at the KpnI site. The same strategy was used to construct pWA362/pWA363, in which the *att* sites are from the MW2 genome, and pWA376/pWA377, in which the *att* sites are from the WBG8318 (WIS) genome. *ccrA*, *ccrB*, *ccrAB*, or *ccrC* was amplified from the genomic DNA of *S. aureus* strains N315, MW2, C98-370, C99-529, J28, J35, FPR3757, and WBG8318 and *Staphylococcus epidermidis* strains SE7 and SE50. PCR products were cloned into the BamHI site of pWA340/pWA341, pWA362/pWA363, or pWA376/pWA377, yielding a set of excision/integration model plasmids. All of the primers used are shown in Table S2 in the supplemental material; all of the plasmids and their characteristics are shown in Table S1 in the supplemental material.

Construction of truncated CcrA and CcrB on model plasmids. To delete the N terminus of CcrA (from amino acids [aa] 119 to 177), two amplified fragments were ligated together after digestion by KpnI: one 0.6-kb fragment amplified with primers *ccrAB*-BamHI-2 and *ccrA*-SR-3 included the promoter and first 118 aa of *ccrA*; the other 1.7-kb fragment of intact *ccrB* was amplified with *ccrB*-SR-1 and *ccrAB*-BamHI-1. The ligated product was amplified with primers *ccrAB*-BamHI-2 and *ccrAB*-BamHI-1 and then inserted into pWA340/pWA341 after it was digested by BamHI, yielding pWA533/pWA534. To delete the C terminus of CcrA (from aa 299 to 450), two amplified fragments were ligated together after digestion by KpnI: one 1-kb fragment amplified with primers *ccrAB*-BamHI-2 and *ccrA*-TR-5 and another 1.7-kb fragment of intact *ccrB* amplified with primers *ccrB*-SR-1 and *ccrAB*-BamHI-1. The ligated product was amplified with primers *ccrAB*-BamHI-1 and *ccrAB*-BamHI-2 and then inserted into pWA340/pWA341 after digestion by BamHI, yielding pWA535/pWA536. To delete the N terminus of CcrB (from aa 1 to 245), two amplified fragments were ligated together after digestion by KpnI: one 1.7-kb fragment including the promoter and intact *ccrA* amplified with primers *ccrAB*-BamHI-2 and *ccrA*-TR-6, and another 1-kb fragment including the last 313 aa of CcrB amplified with primers *ccrB*-SR-9 and *ccrAB*-BamHI-1. The ligated product was amplified with primers *ccrAB*-BamHI-1 and *ccrAB*-BamHI-2 and then inserted into pWA340/pWA341 after it was digested by BamHI, yielding pWA526/pWA527. To get three C-terminal deletion mutants of CcrB (from aa 399 to 543, aa 301 to 543, and aa 241 to 543), three fragments were amplified with three pairs of primers, *ccrAB*-BamHI-2 and *ccrB*-SR-3, *ccrAB*-BamHI-2 and *ccrB*-SR-4, and *ccrAB*-BamHI-2 and *ccrB*-SR-8, respectively. These three fragments were digested by BamHI and inserted into pWA340/pWA341, generating pWA537/pWA538, pWA539/pWA540, and pWA541/pWA542, respectively.

Site-directed mutation of CcrA and CcrB proteins on model plasmids. The primers for site-directed mutagenesis were designed by the online software primerX (http://bioinformatics.org/primerx/cgi-bin/DNA_1.cgi) and are shown in Table S2 in the supplemental material. Site-directed

mutation was performed according to the manufacturer's protocol (Stratagene, La Jolla, CA). Briefly, 25 ng of template plasmid was used to prepare the PCR mixture. The amplification was performed as follows: 95°C for 2 min; 95°C for 30 s, 60°C for 30 s, and 68°C for 6.5 min repeated for 18 cycles; and 68°C for 5 min. Then, 2 μ l of the DpnI restriction enzyme provided with the kit was added to each amplification reaction mixture. The reaction mixtures were incubated at 37°C for 5 min to digest the parental supercoiled dsDNA. The DpnI-treated DNA was transferred into the XL10-Gold ultracompetent cells provided with the kit. The transformants were confirmed by DNA sequencing.

Statistical analysis. The results of independent repeat experiments were averaged, and standard deviations were calculated by the use of Microsoft Excel software. The statistical significance of differences between samples was determined by Student's *t* test, and a *P* value of <0.05 was considered statistically significant. DNA level differences were evaluated densitometrically using ImageJ software. Each experiment was performed at least three times, unless otherwise described in the text.

Structural modeling. The N-terminal domain of the CcrB (amino acids 1 to 205) sequence was submitted to the HHpred interactive server, using default settings, in order to find a suitable template from the Protein Data Bank (PDB) database (22). A list of templates and query-template alignments by hidden Markov matrix (HMM) profiling was generated, with the best being the $\gamma\delta$ resolvase (PDB accession number 1GDT) from *Escherichia coli* (27% sequence identity; E value, $<3.5 \times 10^{-34}$) (23). The E value is a parameter that describes the number of hits expected to be seen by chance, which decreases exponentially as the score of the match increases. In other words, the E value describes the random background noise, with lower values indicating a better match. The resulting alignment of the $\gamma\delta$ resolvase and the CcrB N-terminal domain sequences was provided to the Modeller program for the actual model construction, which is done on the basis of the satisfaction of spatial restraints derived from the template (24). The subsequent CcrB N-terminal domain model was validated using Ramachandran plots and was found to be within acceptable limits (data not shown). The coordinates of the DNA fragment cocrystallized with the $\gamma\delta$ resolvase were then merged with the coordinates of the CcrB N-terminal domain model, and the sequence of the DNA fragment was mutated *in silico* to match the CcrB cognitive DNA sequence using the Discovery Studio Visualizer program (version 3.5; Accelrys, San Diego, CA). After addition of hydrogen atoms, the complete CcrB-DNA model was subjected to energy minimization using the Tripos force field with Gasteiger-Hückel charges and a distance-dependent dielectric to a gradient of 0.01 kcal mol⁻¹ Å⁻¹ in the Sybyl program (version 8.1; Tripos LP, St. Louis, MO).

RESULTS

Recombination frequency in *E. coli* and *S. aureus* determined using plasmid models. The plasmid model was first tested in *E. coli*. Figure 2A demonstrates the N315 CcrAB and N315 *att* site-mediated loss of the 3.1-kb *tetM*-containing fragment from pWA479 (excision) and pWA480 (integration) compared to that in the control plasmids, pWA340 and pWA341, the plasmids with *att* sites and *tetM* but without *ccrAB*. The time course of recombination was monitored through 20 h of growth for pWA479 and pWA480. Plasmid DNA was extracted at 8, 12, 16, and 20 h, digested by BamHI, and separated on a 0.7% agarose gel. As shown in Fig. 2B, the frequency of excision and integration doubled over 20 h, but since the relative frequencies remained approximately the same over this time period, the frequency at 16 h was chosen for comparison for all subsequent studies. In the experiment whose results are illustrated in Fig. 2B, the excision frequency at 16 h was 9.2% \pm 1.6%, while the integration frequency was 3-fold greater at 31.4% \pm 2.7%. Furthermore, DNA sequencing of the smaller plasmids generated following excision showed that 87.5% (7 out of 8) of excision events occurred between *attL* and *attR*,

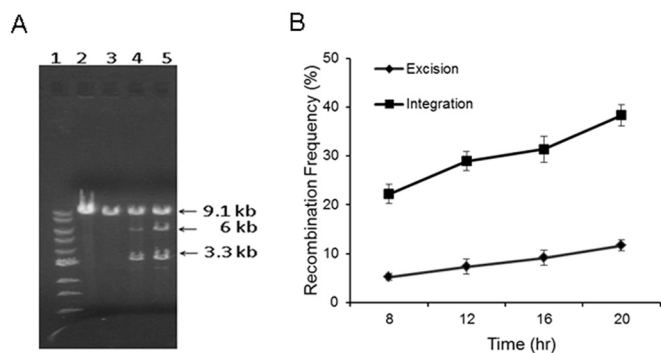


FIG 2 (A) Detection of recombination after plasmid digestion. Lane 1, 1-kb DNA ladder; lane 2, pWA340; lane 3, pWA341; lane 4, pWA479; lane 5, pWA480. All of the plasmids were extracted from *E. coli* TOP10. The plasmids in lanes 2 and 3 are the model plasmids for excision (pWA340) and integration (pWA341). The plasmids in lanes 4 and 5 are the model plasmids following the addition of *ccrAB* and cleavage with BamHI, releasing the 3.3-kb *ccrAB* genes and leaving the plasmid backbone. Recombination frequency was determined by the difference in intensity between the 9.1-kb intact plasmid band and the 6-kb fragment produced when recombination released the tetracycline resistance gene. A complete description of the plasmids is available in Table S1 in the supplemental material. (B) Recombination frequency monitored throughout 8 to 20 h of *E. coli* growth and analyzed for excision (pWA479) and integration (pWA480). The value at each time point represents the mean from four separate experiments, with bars showing the standard deviation.

with only 12.5% (1 out of 8) taking place between *attL* and *attR2*. This is of interest because we have previously shown that excision from *attR* and integration into *attB* require the activity of both CcrA and CcrB, while CcrB alone can mediate excision from an accessory *att* site within SCC_{mec}, *attR2* (6). The model plasmid system shows that excision from *attR* is favored over excision from *attR2*.

To validate the plasmid system in its natural host, *S. aureus*, the model plasmids pWA479 and pWA480 were electroporated into the strain, AW8, from which *attB* was deleted (6) and in which no chromosomal integration could occur. Tetracycline-resistant colonies were picked following electroporation, incubated overnight in TSB without tetracycline, and then grown in 25 ml of fresh TSB to an optical density of 0.6. Following plasmid extraction and BamHI digestion, plasmid DNA was examined on agarose gels as described above for *E. coli*. In the *S. aureus* assay, the excision frequency was $11.0\% \pm 2.8\%$, while the integration frequency was $18.7\% \pm 2.6\%$. In addition, the loss of tetracycline resistance could also be assessed in staphylococci. Strains containing each plasmid were inoculated into fresh TSB without tetracycline on each of three consecutive days to maximize recombination on all plasmid copies. Colonies growing on agar without tetracycline overnight were picked and placed on tetracycline plates, and the number susceptible to tetracycline was determined. Among over 600 colonies, $4.7\% \pm 1.0\%$ of the colonies were tetracycline susceptible for the excision model, but $8.5\% \pm 1.2\%$ were susceptible for the integration model. As described in Materials and Methods, these values are probably underestimates because in some bacterial cells recombination would not have been complete for all plasmid copies, leaving the colony tetracycline resistant. On the basis of both gel examination of the plasmids and the susceptibility of colonies to tetracycline, the integration frequency was approximately twice as high as the excision frequency in *S. aureus*. These results are somewhat lower than the 3-fold increase of the

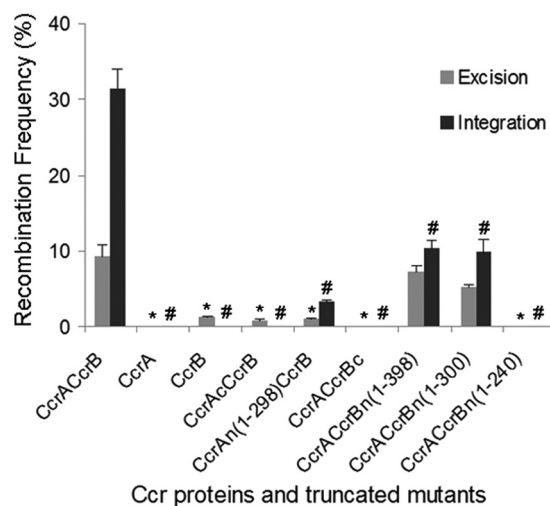


FIG 3 Changes of recombination abilities mediated by CcrAB truncated mutants. CcrA, CcrB, and CcrA CcrB, intact *ccrA*, *ccrB*, and *ccrAB* operons, respectively; CcrAc CcrB, a mutant with deletion of 58 aa of CcrA (from aa 119 to 177) in the *ccr* operon; CcrAn(1–298) CcrB, a mutant with deletion of the C-terminal domain of CcrA (from aa 299 to 450) in the *ccr* operon; CcrA CcrBc, a mutant with deletion of the N-terminal domain of CcrB (from aa 1 to 245) in the *ccr* operon; CcrA CcrBn(1–398), a mutant with deletion of the C-terminal domain of CcrB (from aa 399 to 543) in the *ccr* operon; CcrA CcrBn(1–300), a mutant with deletion of the C-terminal domain of CcrB (from aa 301 to 543) in the *ccr* operon; CcrA CcrBn(1–240), a mutant with deletion of the C-terminal domain of CcrB (from aa 241 to 543) in the *ccr* operon. At least three separate experiments were performed for each mutant. *, $P < 0.05$ versus the excision frequency of wild-type CcrA CcrB; #, $P < 0.05$ versus the integration frequency of wild-type CcrA CcrB.

integration frequency over the excision frequency in *E. coli* but are in the same direction, validating the model in both *E. coli* and the native host. Since the manipulation to determine the frequency of recombination was easier in *E. coli*, most of the following studies were done only in *E. coli*.

Activities of CcrA/CcrB mutants on excision and integration. Although both CcrA and CcrB belong to the large serine recombinase family, they have different contributions to the process of SCC_{mec} excision and integration. Incorporation of either CcrA or CcrB but not both on model plasmids confirmed our previous observations (5) that CcrA alone could not mediate either excision or integration and that CcrB alone mediated excision only and only between *attL* and *attR2* at a low frequency (1.2%; Fig. 3), a result also confirmed by determining the DNA sequence of the deletion junction of plasmids as described above.

CcrA and CcrB have two domains: a conserved N-terminal catalytic domain (referred to as CcrAn and CcrBn, respectively) and a variant large C-terminal domain (referred to as CcrAc and CcrBc, respectively). In order to assess the roles of these two domains in excision and insertion, deletion mutants of CcrA or CcrB were constructed. The recombination frequency was determined as described above. As shown in Fig. 3, a deletion of only 58 aa of CcrA in the N-terminal domain (aa 119 to 177; yielding the CcrAc CcrB mutant) led to the failure of integration. In this mutant, excision took place only between *attL* and *attR2*, a result found only in the complete absence of CcrA. The loss of the C terminus of CcrA [aa 299 to 450; referred to as the CcrAn(1–298) (CcrAn from aa 1 to 298) CcrB mutant] decreased both excision and integration by 90%. Loss of either the N terminus of CcrB (aa 1 to

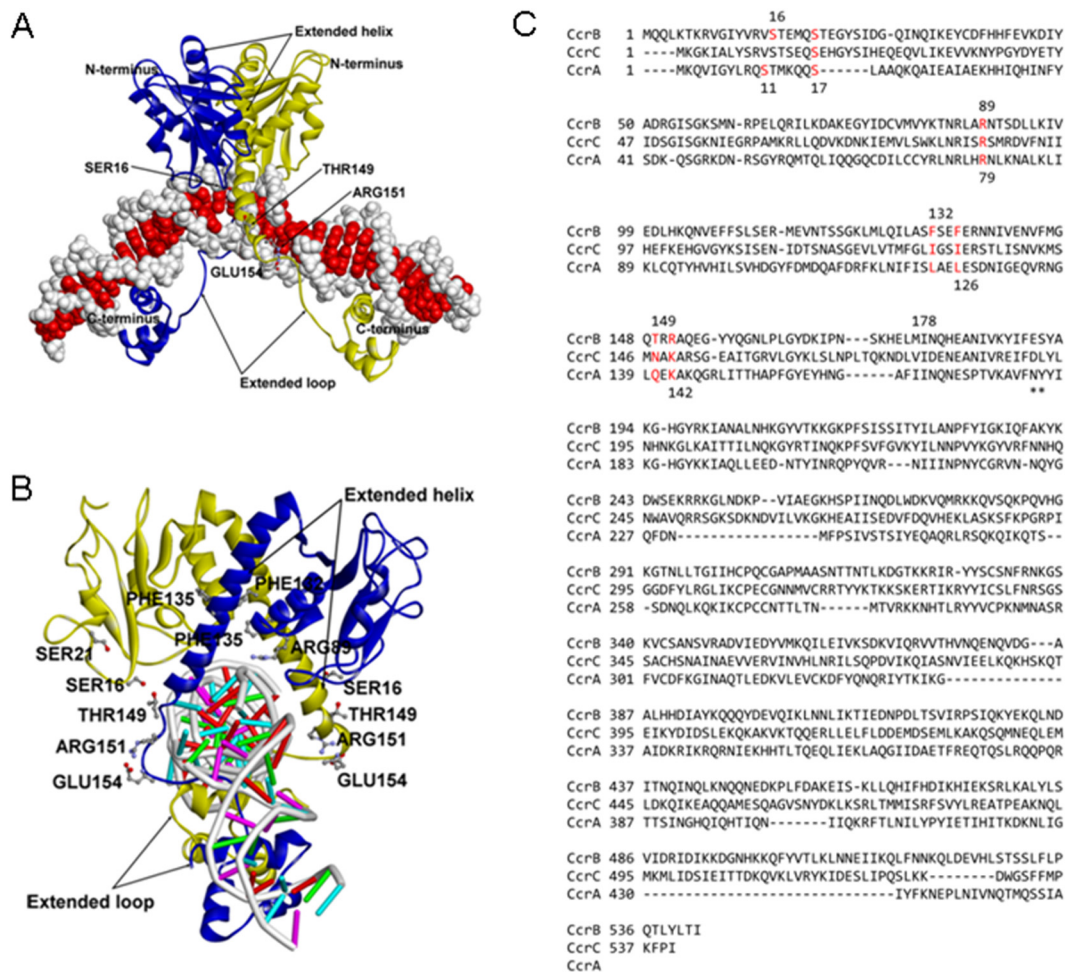


FIG 4 Homology model of the first 205 N-terminal amino acids of CcrB in complex with DNA. (A) Two CcrB N terminus units (in yellow and blue ribbon representations) forming a complex with the DNA fragment (backbone in white and side chains in red, space-filling representation). (B) A 90° rotation of the complex shown in panel A. DNA is in stick representation (backbone in white; side chains of A, C, G, and T in red, magenta, green, and cyan, respectively). (C) Sequence alignment of CcrA, CcrB, and CcrC. Red residues, residues in the N-terminal domain identified from the structural model to be critical for excision and/or integration.

245; referred to as the CcrA CcrBc mutant) or 303 aa of the C terminus [aa 241 to 543; referred to as the CcrA CcrBn(1–240) (CcrBn from aa 1 to 240) mutant] abolished recombination completely, while deletion of only 243 aa or 145 aa of the C terminus [referred to as the CcrA CcrBn(1–300) (CcrBn from aa 1 to 300) mutant and the CcrA CcrB(1–398) (CcrB from aa 1 to 398) mutant, respectively] was less disruptive, resulting in a 22 to 43% decrease in excision and a 70% decrease in integration. Thus, the N-terminal domains of both Ccr proteins are required for recombination, while the C-terminal domain determines catalytic efficiency.

In order to assess the role of specific amino acids in CcrA and CcrB activity, the ~220-aa N-terminal CcrB-DNA complex model (Fig. 4A) was constructed using the published structure of similar serine recombinases (PDB accession number 1GDT) (23). The protein structure of the first 220 aa of CcrB is made up of an N-terminal catalytic domain (NTD) and C-terminal helix-turn-helix DNA-binding domain (CTD) that are linked by an extended helix loop arm. In the complex with DNA, the NTD forms the dimer interface, with the CTD being located in the major groove

of the DNA, while the extended helix loop arm makes contact with the minor groove of the DNA. It is assumed that CcrA and CcrC form structures similar to those formed by CcrB, as suggested by models of the N-terminal portion of these proteins. Critical residues were identified from the structure model and compared among the aligned sequences of CcrA, CcrB, and CcrC, as shown in Fig. 4B and C. Point mutations were introduced into the model plasmids, substituting glycine or alanine for the existing amino acids, and activities were investigated as described above. The effects of the mutations on excision and integration are shown in Fig. 5. S16A, R89G, T149A, and R151G abolished all recombination activity, as predicted because the first three residues are located at the dimer interface, while R151 is likely to be in the DNA-binding loop. Ser16, Arg89, and Thr149 appear to make intersubunit interactions with the opposite subunit (Ser16 to Glu142 and/or Thr149; Arg89 to Asn139), including the flexible long extended helix loop arm (formed by amino acids 123 to 152). Arg151 is located at the extended helix loop arm that connects the NTD and CTD, and although it is not involved in nucleotide binding, it makes a salt bridge/hydrogen bond interac-

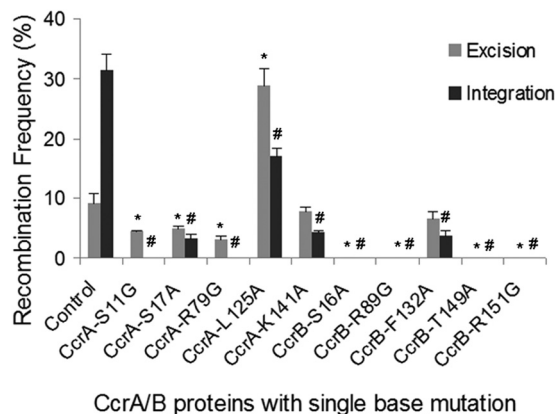


FIG 5 Alteration of catalytic function by introducing single base mutations into CcrAB. For each set, one mutation was introduced into the *ccr* operon. At least three separate experiments were performed for each mutant. *, $P < 0.05$ versus the excision frequency of wild-type CcrA and CcrB; #, $P < 0.05$ versus the integration frequency of wild-type CcrA and CcrB.

tion with Glu154 that should stabilize the loop in the correct orientation for DNA binding. Thus, these mutations could affect not only the dimer stability but also the proper orientation of the extended helix loop arm for DNA binding. Mutations in similar locations in CcrA had less dramatic effects: both S11G (similar to S16 in CcrB) and R79G (similar to R89 in CcrB) abolished integration but only reduced excision compared with that for the control containing both functional proteins. However, the excision occurred only between *attL* and *attR2* and not between *attL* and *attR*, an excision event seen only when CcrB acts alone without any CcrA activity. Thus, it is likely that these two mutations abolished the contribution of CcrA that guided the recombination complex to the usual excision site. The S17A and K142A mutations in CcrA, in locations similar to S21 and R151 in CcrB, respectively, reduced but did not eliminate either excision or inte-

gration. It is interesting that the L125A mutation in CcrA markedly increased the level of excision compared to that for the positive control, with much of the increase in excision occurring between *attL* and *attR2*.

Some of the mutants were examined in *S. aureus* using the change in plasmid size used in *E. coli*, but because of the low recombination frequency and lower yield of plasmid DNA from *S. aureus*, differences were not seen. We therefore evaluated tetracycline susceptibility as a measure of recombination. After 10 days of passage, no tetracycline-susceptible colonies of mutants CcrB S16A and CcrB R89G were seen, confirming the results seen with *E. coli*. The CcrB F132 mutation produced $1.8\% \pm 0.3\%$ tetracycline-susceptible colonies for excision and $1.0\% \pm 0.2\%$ for integration, mirroring, and in the same direction as, the difference seen for *E. coli*. Similarly, the CcrA S11G and R79G mutations produced no tetracycline-susceptible colonies for the integration model but $0.7\% \pm 0.2\%$ and $0.6\% \pm 0.1\%$ tetracycline-susceptible colonies, respectively, for the excision model. Thus, while the results for *S. aureus* were not as robust as those for *E. coli*, they precisely duplicated the changes in both excision and integration observed in the heterologous host.

Activities of CcrA and CcrB from MRSA and MRSE strains.

An earlier study from the Archer lab showed that the *ccrAB* genes found in SCC_{mec} types II and IV varied by up to 5% at the amino acid level, yet all of the tested recombinases mediated SCC_{mec} excision in MRSA strains (25). To further identify the activities of CcrAB from a panel of strains, the *ccrAB* genes and the *ccrC* gene of seven MRSA strains and two methicillin-resistant *S. epidermidis* (MRSE) strains were examined using the model plasmid system to determine their abilities to mediate excision and integration, and the results were compared with those presented above for N315 (Fig. 6A). CcrC and most CcrAB proteins catalyzed integration at a higher frequency than they did excision, with the frequency of integration exceeding the frequency of excision by from 1.3-fold (FPR3757) to 10-fold (J28). The exception was CcrAB from MW2,

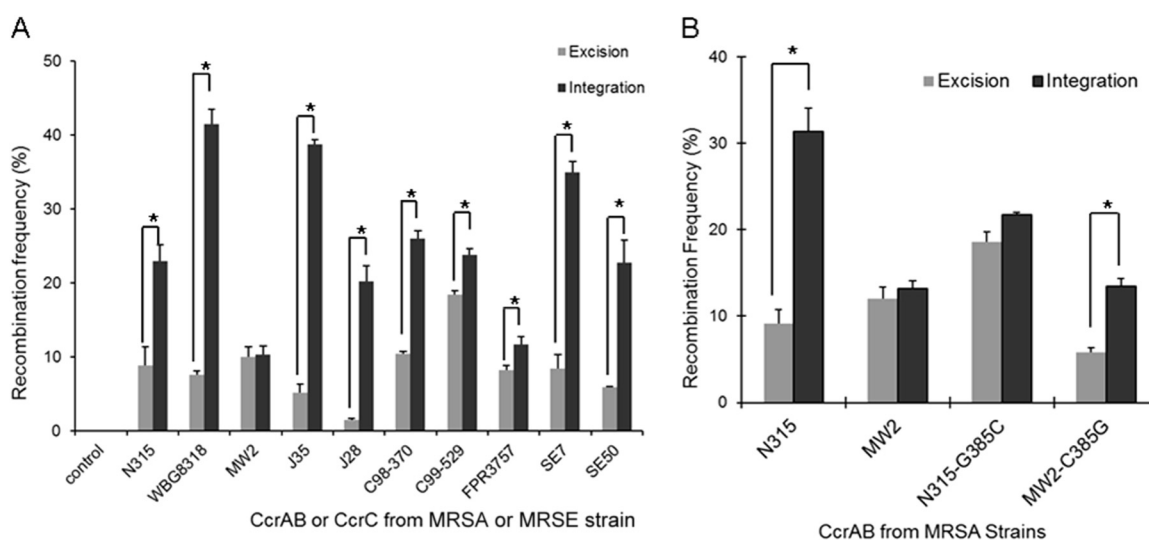


FIG 6 (A) Excision and integration catalyzed by CcrAB or CcrC (WBG8318) from strains carrying SCC_{mec} types II, IV, and V in *E. coli* TOP10 cells. The *ccrAB* or *ccrC* genes were from a series of MRSA or MRSE strains which are described in Table S1 in the supplemental material. Comparison of the amino acid sequences of the CcrAB proteins from the *S. aureus* strains described here can be found in Fig. S1 in the supplemental material. (B) Excision and integration catalyzed by CcrAB from N315 and MW2 with a change of aa 385 in CcrB. At least three repeats were done for each set of CcrA and CcrB proteins. *, $P < 0.01$ for integration versus excision.

in which excision and integration frequencies were the same. The protein sequences of CcrAB in each of the *S. aureus* and *S. epidermidis* strains for which the results are shown in Fig. 6A were compared (see Fig. S1 in the supplemental material). For CcrA, none of the amino acid differences were seen only in MW2. However, there were nine amino acid changes in the CcrB sequence of MW2 not seen in the CcrB sequences of the other strains. All but one (E73D) of the changes were in the carboxy terminus (see Fig. S1 in the supplemental material). All of the changes were relatively conservative, except for the change at aa 385, at which glycine was changed to cysteine in MW2. We repaired the mutation in MW2 from a cysteine to a glycine and exchanged the glycine for the mutant cysteine in N315, yielding the result seen in Fig. 6B. The MW2 C385G change reduced excision by 47%, causing integration to exceed excision by 2.32-fold, a difference similar to that seen in N315. In contrast, the G385C exchange in N315 both decreased integration and increased excision so that the recombination frequency seen in mutant N315 resembled the recombination frequency seen in MW2. These results suggest both that this is a critical mutation that affects the direction of recombination and that the carboxy terminus of CcrB plays an important role in determining the frequency of integration versus that of excision.

DISCUSSION

In the current study, we have demonstrated that the recombinational activity of CcrA and CcrB favors integration over excision, demonstrated by plasmid models in both *S. aureus* and *E. coli* and in a panel of clinical *S. aureus* and *S. epidermidis* isolates. This is consistent with our observation that spontaneous excision *in vitro* is an extremely rare event but does not support either one of the two potential explanations: rare excision associated with a stably integrated element, as postulated by others (18, 26), or frequent excision followed by immediate reintegration, events associated with more instability of the integrated element. The observation that in one isolate, *S. aureus* MW2, plasmid-modeled excision and integration were equal yet spontaneous excision *in vitro* was at the same low rate seen for other isolates (Wang, unpublished) suggests that excision with reinsertion may be occurring in some isolates. Our previous data have shown that excision can be favored over integration when the concentrations of CcrB and CcrA are increased by their inclusion on a high-copy-number plasmid or driven by an inducible promoter (5). Thus, the concentrations and ratios of the two recombinases are critical for determining stable integration versus excision, and anything that increases *ccrAB* expression may favor excision. A previous study found that the *ccrAB* promoter was active in only a small percentage of cells in a population and that the activity, determined by unknown genes elsewhere in the chromosome, was strain dependent (26). An earlier report suggesting that various antibiotics increased *ccrAB* expression (27) and our observation that some isolates colonizing patient nares contained excised variants occurring at rates higher than those seen *in vitro* may point to *in vivo* conditions that could favor excision over integration (28). While the current study suggests that under stable *in vitro* conditions integration is favored and, thus, that passage of SCCmec to progeny is the rule, excision is likely to occur under certain conditions in order for horizontal transmission of SCCmec to occur.

CcrA and CcrB are large serine recombinases that consist of an N-terminal domain and a C-terminal domain. The model that we generated (Fig. 4) is based on the similarity of the N terminus

(amino acid 1 to ~220) to smaller serine recombinases (23) and contains both a catalytic domain and the DNA-binding domain. The function of the C terminus (amino acids ~220 to 543 for CcrB and ~210 to 450 for CcrA) is unknown. However, as shown in Fig. 3, while an N-terminal deletion of either CcrA or CcrB abolishes both excision and integration, a C-terminal deletion does not eliminate but markedly reduces both activities. Thus, the C terminus seems to have a role in the efficiency of recombination. Rutherford et al. (29) recently reported the X-ray structure of the C-terminal domain of listeria phage integrase bound to its *attP* half site, which, in conjunction with recombination and DNA-binding experimental data, led the authors to propose a model for the recombination pathway that explains how large serine recombinases regulate site selectivity and directionality. Interestingly, using the HHpred structural homology program (22), we found the CTD of CcrB to be structurally homologous to the CTD of listeria phage integrase. Moreover, using the C-terminal amino acid sequence of CcrB for a search, we also identified a recombinase, the zinc beta ribbon domain from the Pfam database (30), which is known to bind DNA. These observations lead us to speculate that the CTD of CcrB might also associate with the DNA half site, orienting it in the correct position for integration/excision operations conducted through the NTD.

An understanding of the dynamics of SCCmec excision and integration could have therapeutic implications. We have previously shown (31) that when isogenic MRSA strains with and without SCCmec compete *in vitro*, the strain without SCCmec is more fit, becoming the predominant species in the culture within 4 days. Thus, if SCCmec excision could be induced to exceed integration *in vivo*, the excised variant may be more fit and become predominant, converting an MRSA strain into a susceptible strain, broadening therapeutic options.

ACKNOWLEDGMENTS

Nucleic acid sequence determination was performed at the Virginia Commonwealth University Nucleic Acid Research Facility.

This study was supported by grant 5R01AI035705-20 from the National Institute of Allergy and Infectious Diseases.

REFERENCES

- Crossley K, Jefferson K, Archer GL, Fowler VG, Jr (ed). 2009. Staphylococci in human disease. Wiley-Blackwell, West Sussex, United Kingdom.
- Ito T, Hiramatsu K, Oliveira DC, de Lencastre H, Zhang K, Westh H, O'Brien F, Giffard PM, Coleman D, Tenover FC, Boyle-Vavra S, Skov RL, Enright MC, Kreiswirth B, Ko KS, Grundmann H, Laurent F, Sollid JE, Kearns AM, Goering R, John JF, Daum R, Soderquist B, International Working Group on the Classification of Staphylococcal Cassette Chromosome Elements (IWG-SCC). 2009. Classification of staphylococcal cassette chromosome *mec* (SCCmec): guidelines for reporting novel SCCmec elements. *Antimicrob Agents Chemother* 53:4961–4967. <http://dx.doi.org/10.1128/AAC.00579-09>.
- Ito T, Ma XX, Takeuchi F, Okuma K, Yuzawa H, Hiramatsu K. 2004. Novel type V staphylococcal cassette chromosome *mec* driven by a novel cassette chromosome recombinase, *ccrC*. *Antimicrob Agents Chemother* 48:2637–2651. <http://dx.doi.org/10.1128/AAC.48.7.2637-2651.2004>.
- Katayama Y, Ito T, Hiramatsu K. 2000. A new class of genetic element, staphylococcus cassette chromosome *mec*, encodes methicillin resistance in *Staphylococcus aureus*. *Antimicrob Agents Chemother* 44:1549–1555. <http://dx.doi.org/10.1128/AAC.44.6.1549-1555.2000>.
- Wang L, Archer GL. 2010. Roles of CcrA and CcrB in excision and integration of staphylococcal cassette chromosome *mec*, a *Staphylococcus aureus* genomic island. *J Bacteriol* 192:3204–3212. <http://dx.doi.org/10.1128/JB.01520-09>.
- Wang L, Safo M, Archer GL. 2012. Characterization of DNA sequences

- required for the CcrAB-mediated integration of staphylococcal cassette chromosome *mec*, a *Staphylococcus aureus* genomic island. *J Bacteriol* 194:486–498. <http://dx.doi.org/10.1128/JB.05047-11>.
7. Kuhstoss S, Rao RN. 1991. Analysis of the integration function of the streptomycete bacteriophage ϕ C31. *J Mol Biol* 222:897–908. [http://dx.doi.org/10.1016/0022-2836\(91\)90584-S](http://dx.doi.org/10.1016/0022-2836(91)90584-S).
 8. Smith MCM, Brown WRA, McEwan AR, Rowley PA. 2010. Site-specific recombination by ϕ C31 integrase and other large serine recombinases. *Biochem Soc Trans* 38:388–394. <http://dx.doi.org/10.1042/BST0380388>.
 9. Bibb LA, Hancox MI, Hatfull GF. 2005. Integration and excision by the large serine recombinase ϕ CpRv1 integrase. *Mol Microbiol* 55:1896–1910. <http://dx.doi.org/10.1111/j.1365-2958.2005.04517.x>.
 10. Christiansen B, Brøndsted L, Vogensen FK, Hammer K. 1996. A resolvase-like protein is required for the site-specific integration of the temperate lactococcal bacteriophage TP901-1. *J Bacteriol* 178:5164–5173.
 11. Ghosh P, Bibb LA, Hatfull GF. 2008. Two-step site selection for serine-integrase-mediated excision: DNA-directed integrase conformation and central dinucleotide proofreading. *Proc Natl Acad Sci U S A* 105:3238–3243. <http://dx.doi.org/10.1073/pnas.0711649105>.
 12. Ghosh P, Wasil LR, Hatfull GF. 2006. Control of phage Bxb1 excision by a novel recombination directionality factor. *PLoS Biol* 4:e186. <http://dx.doi.org/10.1371/journal.pbio.0040186>.
 13. Kim AI, Ghosh P, Aaron MA, Bibb LA, Jain S, Hatfull GF. 2003. Mycobacteriophage Bxb1 integrates into the *Mycobacterium smegmatis* *groEL1* gene. *Mol Microbiol* 50:463–473. <http://dx.doi.org/10.1046/j.1365-2958.2003.03723.x>.
 14. Lyras D, Adams V, Lucet I, Rood JI. 2004. The large resolvase TnpX is the only transposon-encoded protein required for transposition of the Tn4451/3 family of integrative mobilizable elements. *Mol Microbiol* 51:1787–1800. <http://dx.doi.org/10.1111/j.1365-2958.2003.03950.x>.
 15. Wang H, Mullany P. 2000. The large resolvase TndX is required and sufficient for integration and excision of derivatives of the novel conjugative transposon Tn5397. *J Bacteriol* 182:6577–6583. <http://dx.doi.org/10.1128/JB.182.23.6577-6583.2000>.
 16. Wang H, Smith MCM, Mullany P. 2006. The conjugative transposon Tn5397 has a strong preference for integration into its *Clostridium difficile* target site. *J Bacteriol* 188:4871–4878. <http://dx.doi.org/10.1128/JB.00210-06>.
 17. Misiura A, Pigli YZ, Boyle-Vavra S, Daum RS, Boocock MR, Rice PA. 2013. Roles of two large serine recombinases in mobilizing the methicillin-resistance cassette SCC_{mec}. *Mol Microbiol* 88:1218–1229. <http://dx.doi.org/10.1111/mmi.12253>.
 18. Stojanov M, Moreillon P, Sakwinska O. 2012. Dynamics of excision of the staphylococcal cassette chromosome *mec* (SCC_{mec}) in methicillin-resistant *Staphylococcus aureus* (MRSA), abstr C1-1746, p 169. Abstr 52nd Intersci Conf Antimicrob Agents Chemother, San Francisco, CA. American Society for Microbiology, Washington, DC.
 19. Schenk S, Laddaga RA. 1992. Improved method for electroporation of *Staphylococcus aureus*. *FEBS Microbiol Lett* 94:1333–1338.
 20. Stephenson FH. 2010. Recombinant DNA, p 313–368. *In* Calculations for molecular biology and biotechnology. Academic Press, Amsterdam, Netherlands.
 21. Charpentier E, Anton AI, Barry P, Alfonso B, Fang Y, Novick RP. 2004. Novel cassette-based shuttle vector system for gram-positive bacteria. *Appl Environ Microbiol* 70:6076–6085. <http://dx.doi.org/10.1128/AEM.70.10.6076-6085.2004>.
 22. Soding J, Biegert A, Lupas AN. 2005. The HHpred interactive server for protein homology detection and structure prediction. *Nucleic Acids Res* 33(Web Server issue):W244–W248.
 23. Yang W, Steitz TA. 1995. Crystal structure of the site-specific recombinase gamma delta resolvase complexed with a 34 bp cleavage site. *Cell* 82:193–207. [http://dx.doi.org/10.1016/0092-8674\(95\)90307-0](http://dx.doi.org/10.1016/0092-8674(95)90307-0).
 24. Fiser A, Sali A. 2003. Modeller: generation and refinement of homology-based protein structure models. *Methods Enzymol* 374:461–491.
 25. Noto MJ, Archer GL. 2006. A subset of *Staphylococcus aureus* strains harboring staphylococcal cassette chromosome *mec* (SCC_{mec}) type IV is deficient in CcrAB-mediated SCC_{mec} excision. *Antimicrob Agents Chemother* 50:2782–2788. <http://dx.doi.org/10.1128/AAC.00032-06>.
 26. Stojanov M, Sakwinska O, Moreillon P. 2013. Expression of SCC_{mec} cassette chromosome recombinases in methicillin-resistant *Staphylococcus aureus* and *Staphylococcus epidermidis*. *J Antimicrob Chemother* 68:749–757. <http://dx.doi.org/10.1093/jac/dks494>.
 27. Higgins PG, Rosato AE, Seifert H, Archer GL, Wisplinghoff H. 2009. Differential expression of *ccrA* in methicillin-resistant *Staphylococcus aureus* strains carrying staphylococcal cassette chromosome *mec* type II and IVa elements. *Antimicrob Agents Chemother* 53:4556–4558. <http://dx.doi.org/10.1128/AAC.00395-09>.
 28. Boundy S, Zhao Q, Fairbanks C, Folgosa L, Climo MW, Archer GL. 2012. Spontaneous SCC_{mec} excision in *Staphylococcus aureus* nasal carriers. *J Clin Microbiol* 50:469–471. <http://dx.doi.org/10.1128/JCM.01063-11>.
 29. Rutherford K, Yuan P, Perry K, Sharp R, Van Duyn GD. 2013. Attachment site recognition and regulation of directionality by the serine integrases. *Nucleic Acids Res* 41:8341–8356. <http://dx.doi.org/10.1093/nar/gkt580>.
 30. Finn RD, Bateman A, Clements J, Coggill P, Eberhardt RY, Eddy SR, Heger A, Hetherington K, Holm L, Mistry J, Sonnhammer ELL, Tate J, Punta M. 2014. The Pfam protein families database. *Nucleic Acids Res* 42(Database issue):D222–D230. <http://dx.doi.org/10.1093/nar/gkt1223>.
 31. Noto MB, Fox PM, Archer GL. 2008. Spontaneous deletion of the methicillin resistance determinant, *mecA*, partially compensates for the fitness cost associated with high level vancomycin resistance in *Staphylococcus aureus*. *Antimicrob Agents Chemother* 52:1221–1229. <http://dx.doi.org/10.1128/AAC.01164-07>.